



**HAL**  
open science

# A Comprehensive Study on Effect of Biofuel Blending Obtained from Hydrothermal Liquefaction of Olive Mill Waste Water in Internal Combustion Engine

Fatma Zohra Aklouche, Loubna Hadhoum, Khaled Loubar, Mohand Tazerout

► **To cite this version:**

Fatma Zohra Aklouche, Loubna Hadhoum, Khaled Loubar, Mohand Tazerout. A Comprehensive Study on Effect of Biofuel Blending Obtained from Hydrothermal Liquefaction of Olive Mill Waste Water in Internal Combustion Engine. *Energies*, 2023, 16, 10.3390/en16062534 . hal-04107358

**HAL Id: hal-04107358**

**<https://hal.science/hal-04107358>**

Submitted on 26 May 2023

**HAL** is a multi-disciplinary open access archive for the deposit and dissemination of scientific research documents, whether they are published or not. The documents may come from teaching and research institutions in France or abroad, or from public or private research centers.

L'archive ouverte pluridisciplinaire **HAL**, est destinée au dépôt et à la diffusion de documents scientifiques de niveau recherche, publiés ou non, émanant des établissements d'enseignement et de recherche français ou étrangers, des laboratoires publics ou privés.

## Article

# A Comprehensive Study on Effect of Biofuel Blending Obtained from Hydrothermal Liquefaction of Olive Mill Waste Water in Internal Combustion Engine

Fatma Zohra Aklouche, Loubna Hadhoum, Khaled Loubar \*  and Mohand Tazerout

IMT Atlantique, Energy Systems and Environment Department, GEPEA, UMR CNRS 6144, 04 Rue Alfred Kastler, CS 20722, 44307 Nantes, France

\* Correspondence: khaled.loubar@imt-atlantique.fr

**Abstract:** The production of biofuel from olive mill wastewater (OMWW) may be one of the promising techniques for use in diesel engines. In this study, biofuel was produced from the hydrothermal liquefaction of OMWW using a methanol-water co-solvent. Biofuel blends of 10% (B10), 20% (B20) and 30% (B30) by volume of biofuel, were prepared. The chemical and physical properties of biofuel blends are mostly similar to those of conventional diesel fuel. The engine speed was kept constant (1500 rpm) throughout the tests under different engine loads (25, 50, 75 and 100%). The effects of biofuel-diesel blends on exhaust emissions and engine performance were investigated. The results show that the in-cylinder pressure follows almost the same trend for all fuels. However, at high loads, with increasing biofuel blend, the combustion duration tends to become longer. The B10 blend provided close results to diesel fuel in terms of performance and polluting emissions. Moreover, the use of B10 resulted in reduced emission levels, with 11% of unburned hydrocarbons, 12% of particles and 26% of carbon dioxide compared to the other blends.

**Keywords:** olive mill wastewater; biofuel blend; diesel engine; combustion analysis; pollutant emissions



**Citation:** Aklouche, F.Z.; Hadhoum, L.; Loubar, K.; Tazerout, M. A Comprehensive Study on Effect of Biofuel Blending Obtained from Hydrothermal Liquefaction of Olive Mill Waste Water in Internal Combustion Engine. *Energies* **2023**, *16*, 2534. <https://doi.org/10.3390/en16062534>

Academic Editors: Georgios Mavropoulos, E.C. Andritsakakis and Roussos G. Papagiannakis

Received: 20 January 2023

Revised: 27 February 2023

Accepted: 6 March 2023

Published: 7 March 2023



**Copyright:** © 2023 by the authors. Licensee MDPI, Basel, Switzerland. This article is an open access article distributed under the terms and conditions of the Creative Commons Attribution (CC BY) license (<https://creativecommons.org/licenses/by/4.0/>).

## 1. Introduction

In recent years, the growing concerns about the availability of fossil fuel resources have increased interest in the search for alternative fuels [1,2]. It has been accelerated owing to the increasing energy demand and limited fossil fuel reserves. The use of biomass as a renewable energy source to produce second-generation biofuels has been proposed as a promising solution to reduce greenhouse gas emissions and minimize the competition between food and fuel production [3].

The United States, Brazil, and the European Union account for approximately 90% of global biofuel production. However, if development programs in other nations like Malaysia and China are successful, production could become more widely distributed. In these countries, corn, sugar, and vegetable oils are the primary raw materials used for biofuel production [4].

Biomass obtained from organic waste, such as sewage sludge and sorted domestic organic waste, exists in different forms and is highly perishable. This is due to their high moisture content ranging from 50 to 80% [5]. In the case where these raw materials are not properly disposed of, they often cause serious environmental problems.

The industrial extraction of olive oil is associated with certain negative effects on the environment such as pollution of water bodies, atmospheric emissions, soil contamination and underground seepage, as a result of the production of a large amount of liquid and solid wastes [6]. The generated liquid waste called olive mill wastewater (OMWW) varies between 0.3 and 1.1 m<sup>3</sup> per ton of processed olives, depending on the extraction technology employed [7]. OMWW is acidic and contains many suspended solids, organic compounds and high levels of pollutants such as heavy metals. In addition, the high concentration

of phenolic compounds contained in OMWW could have a severe environmental impact. Their strong antioxidant activity is primarily attributed to their ability to donate the hydrogen atom of the phenolic hydroxyl group to free radicals [8]. In this context, if properly converted, OMWW could be considered a sustainable feedstock for biofuel production due to lack of the competition with food and feed use [9]. According to the literature, few studies have been carried out on the recovery of energy from this waste by thermochemical conversion. Various processes such as gasification [10], pyrolysis [11], combustion [12] and hydrothermal carbonization [13] have been investigated for OMWW conversion leading to different types of chemicals. However, the high humidity of OMWW (more than 80%) represents the main limitation for processes such as pyrolysis or combustion because of the high energy consumption. Among the conversion techniques, which are suitable for the production of biofuels, is the hydrothermal liquefaction (HTL) process. It is the most practical since it does not require the drying of the biomass upstream. Targeting the production of liquid biofuels, the HTL process is carried out in general at moderate temperatures (250 and 400 °C) under pressure conditions ranging from 5 to 24 MPa [1,13]. The liquefaction mechanism includes several consecutive steps, which start when the biomass is depolymerized to form water-soluble monomers. This step is followed by the degradation of monomer by deamination, dehydration and decarboxylation reactions [14]. After that, the reactive fragments are recombined to form the bio-oil. However, if the reaction time is prolonged further, polymerization reactions accrued to form char [5,15]. Therefore, the HTL process was favored for the conversion of OMWW to biofuel [9,16]. In addition, it was reported that the higher heating value (HHV) of biofuel obtained from HTL of OMWW using methanol-water co-solvent was 43.20 MJ/kg resulting in better physicochemical properties [9]. Despite the growing interest in the use of OMWW as a potential feedstock for biofuel production, only a limited number of studies have investigated the application of other technologies for this purpose. Among them, Haddad et al. [17] conducted a study on the pyrolysis of impregnated sawdust with OMWW and reported a biofuel yield of approximately 25%. In addition, Elleuch et al. [18] have used OMWW sludge as a feedstock to produce upgraded biofuel through a combination of pyrolysis and the esterification process.

The interest in biofuel production for internal combustion engines has increased sharply since the 1970s. Burning fossil fuels results in the emission of carbon dioxide and other greenhouse gases, which in turn trap heat in our atmosphere, causing them to be the main contributors to global warming and climate change. However, renewable hydrocarbon biofuels produced from biomass sources are the only alternative energy source for transportation fuel. Since they meet the same ASTM fuel quality standards as the petroleum fuels they replace, these biofuels can be used in existing engines and infrastructure.

Generally, when using biofuel/diesel blends, the alternative fuel is externally blended with diesel using different blending ratios. Nevertheless, the dual-injection strategy offers greater flexibility when using biofuels. This is due to the variation of blending ratios which can be used by separately injecting different quantities into the engine [19].

The produced biofuels have different properties owing to the feedstock and thermochemical process used. Nonetheless, there are still some relevant problems to be addressed regarding the use of biofuel blends on diesel engines.

Diesel engines are a significant source of various types of air pollutants, including particulate matter (PM), nitrogen oxides (NO<sub>x</sub>), carbon monoxide (CO), carbon dioxide (CO<sub>2</sub>), and other harmful compounds. Engine development is increasingly focused on reducing emissions due to the heightened awareness of environmental pollution and the stricter government regulations on exhaust emissions. The reduction of engine emissions has become a crucial research objective to address these concerns. During the last years, experimental studies about using biofuel blends in diesel engines have appeared in numerous published papers which are available in the literature [20–23]. It was reported that an increase in biofuel percentage in fuel blends results in a decrease in emissions of carbon monoxide (CO), smoke/particulate matter (PM), and unburned hydrocarbons, as

well as a moderate increase in nitrogen oxides (NO<sub>x</sub>) emissions during both steady-state and transient operation [24,25]. Recently, Karthikeyan et al. [26] investigated the effect of blends of biofuel/diesel fuel (B20, B50, B75 and B100) on the performance of diesel engines. This biofuel was produced from *S. Marginatum* macroalgae. It was observed that B20 (20% of biofuel in the blend) performed more effective combustion at high loads as well. Similarly, Kumar et al. [27] conducted diesel engine tests using a biofuel derived from the transesterification of *Jatropha* oil, by varying fuel injection pressure. They reported the thermal efficiency of the biofuel-powered engine increased at maximum load as the fuel injection pressure increased. This was explained by an enhancement of the combustion process due to the oxygen content in the biofuel [28]. In addition, biocrude from hydrothermal conversion of *Pinus radiata* wood floor was investigated by blending with diesel for engine experiments, at an engine speed of 2000 rpm [29]. Five engine loads (0%, 25%, 50%, 75% and 100%) were considered. Authors reported a maximum of 13% higher specific total hydrocarbon emissions with a 20% blend. Additionally, compared to diesel fuel, particulate matter emissions were lower for all biofuel blends.

According to the literature review above, no study has yet investigated the utilization of biofuel derived from the HTL process using methanol-water co-solvent in stationary generation applications using diesel engines. This motivates our research to explore the performance of biofuel obtained from HTL of OMWW on engine performance.

The current study aims to investigate the effect of biofuel blended with diesel fuel on existing engine emissions. The biofuel was produced from OMWW using the HTL process. The physicochemical properties of blends were measured in order to determine the quality of fuel mixtures. Moreover, combustion and exhaust gas emissions have been investigated with neat diesel fuel and biofuel/diesel blends based on experimental engine tests. Engine performance and emissions for three different blends (10%, 20% and 30% by volume) were examined. The analysis focuses on examining how the use of biofuel blends affects the exhaust emissions of a diesel engine operating at various engine loads. Specifically, the emissions of CO, CO<sub>2</sub>, NO<sub>x</sub> and HC are documented and then compared with diesel fuel.

## 2. Materials and Methods

### 2.1. Biofuel Production

In this study, the feedstock used was OMWW, which was obtained from a traditional oil mill located in the northern region of Algeria. The diesel fuel used in the experiment was procured from a gas station. The raw material was subjected to analyzes and physicochemical properties (proximate, biochemical and elemental analysis, etc.) were determined and depicted in Table 1.

**Table 1.** Analysis of OMWW Composition through proximate, ultimate, and chemical composition.

Proximate Analysis (wt.%)		Ultimate Analysis (On Dry Basis, wt.%)		Chemical Composition (On Dry Basis, wt.%)	
Moisture, as received	78.50	C	46.87	Hemicellulose	36.90
Ash (on a dry basis)	21.87	H	6.88	Cellulose	19.47
Volatiles	58.70	N	2.40	Lignin	28.55
Fixed carbon	24.26	S	n.d <sup>b</sup>	Fat, as received	14.30
		O <sup>a</sup>	21.98	HHV (MJ/kg)	24.26

<sup>a</sup> By difference. <sup>b</sup> Not detected.

The experiments of liquefaction were carried out in an unstirred cylindrical batch reactor (volume of 998 mL), which was made of stainless steel. In our previous work, methanol was utilized as a co-solvent in a 50/50% ratio with water [9]. For each experiment, methanol-water co-solvent was blended with OMWW (as received), containing 32 wt.% of dry biomass, to make 100 g of feedstock. In a typical run, the reactor was filled with OMWW at the optimal ratio of 50/50 (% w/w) of methanol-water co-solvent [9]. Residue

air was removed by purging  $N_2$  for 10 min. When the temperature reached the reaction temperature of  $280\text{ }^\circ\text{C}$ , it was maintained for 30 min as reaction time.

To effectively separate the bio-oil from the water phase, the gaseous product was collected from the reactor headspace into a gas-sampling bag and analyzed using a Micro-GC analyzer. To open the reactor, the valve assembly was removed, and the reaction content was carefully retrieved. The resulting mixture was then transferred to a vessel for the separation process. The reactor was subsequently cleaned three times with  $\text{CH}_2\text{Cl}_2$  to ensure the complete retrieval of all contents. Roughly 250 mL of  $\text{CH}_2\text{Cl}_2$  (including the washing solution) was added to the reaction mixture, which was then subjected to vacuum filtration through a Buchner funnel. The liquid phase was transferred to a separatory funnel, where the solvent fraction was separated from the aqueous phase. Furthermore, the solvent was eliminated under vacuum using a rotary evaporator, and the remaining product was classified as the “biofuel” fraction. The solid residue was dried at  $105\text{ }^\circ\text{C}$  for 12 h in an oven, and its weight and composition were analyzed. The aqueous phase was dried at  $70\text{ }^\circ\text{C}$  for 12 h in the oven, and the resulting material was classified as water-soluble products. Further information on optimizing biofuel production was reported in previous work [9].

## 2.2. Physicochemical Properties of Biofuel Blends

In order to investigate the engine performance and pollutant emissions of a diesel engine utilizing the produced biofuel, various volume proportions of biofuel/diesel blend fuels were prepared. For crude biofuel, 70:30 (v/v, B30), 20:80 (v/v, B20), 10:90 (v/v, B10), in addition to 100% 0# diesel (B0), which served as the baseline (reference) fuel.

Fuel properties play a crucial role in the determination of the quality of fuel blending and the combustion process. Researchers often highlight properties such as calorific value, viscosity, flash point and cetane number to describe the effects of biofuel additives on the combustion process, performance, and emission characteristics of a diesel engine [30,31].

Fuel properties are crucial in determining the quality of fuel blends and the combustion process. Researchers have consistently identified properties such as calorific value, flash point, density, cetane number, and viscosity as key factors in describing the effects of biofuel blending on the performance, emissions, and combustion of a diesel engine [32,33]. In this fact, Figure 1 shows the physicochemical properties of conventional diesel fuel and biofuel/diesel blends, which are determined based on the ASTM standard.

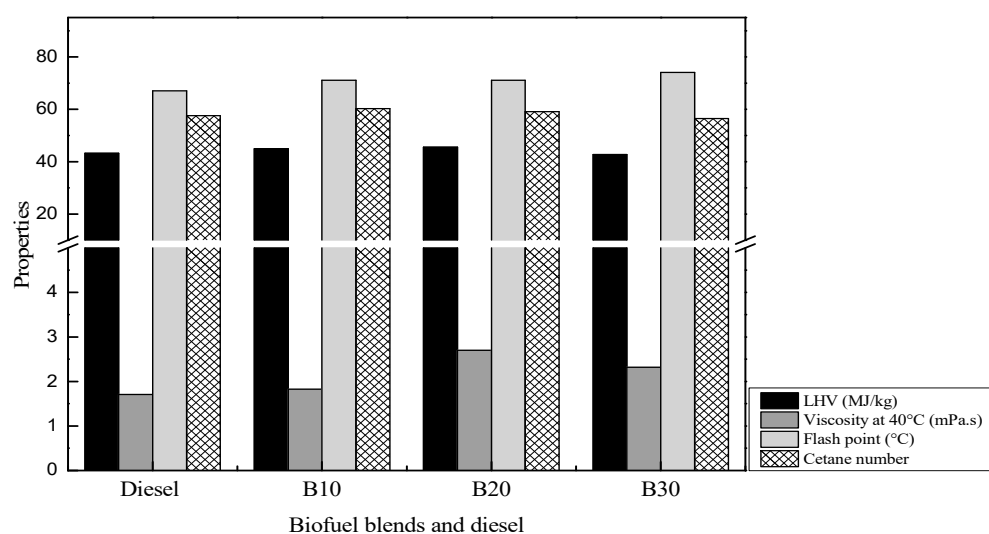


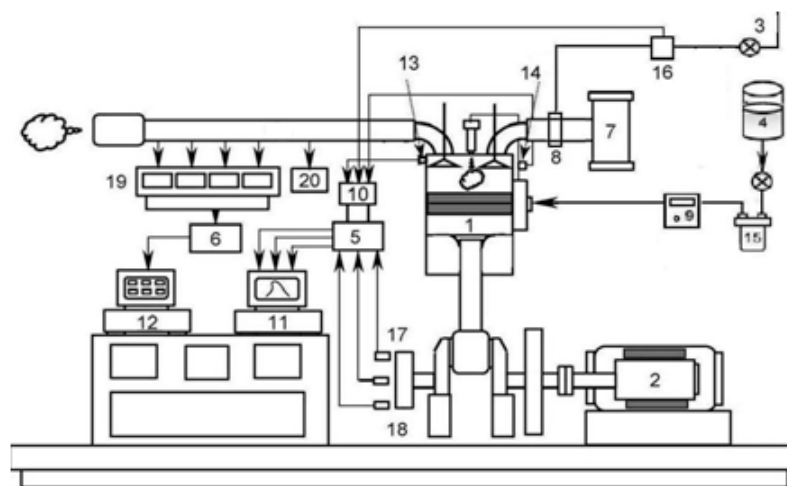
**Figure 1.** Physicochemical properties of biofuel/diesel blends.

The physicochemical properties indicate the good quality of biofuel blended for its combustion in the diesel engine by its density values (ranging from  $838$  to  $848\text{ kg/m}^3$ ) close to that of diesel ( $852\text{ kg/m}^3$ ). Viscosity plays a similar role as density to define the quality

of atomization, penetration through the injection system, and the size of the fuel droplet are all factors that influence the performance and emissions of an engine, and therefore affect the overall quality of combustion. The increase of diesel content in blends led to enhancing the viscosity of the biofuel blends. In addition, the cetane number is a significant property that affects the quality of fuel combustion in diesel engines. Indeed, a low cetane number induces a longer ignition delay and an increased tendency to knock. The biofuel blends have a cetane number close to conventional diesel varying between 57 and 60. Moreover, the blend's flash points, indicating the presence of volatile materials, are similar to that of diesel fuel. This property does not greatly affect the quality of combustion. Nevertheless, with regard to the transport, storage and handling of fuel, this parameter is essential. The lower heating value (LHV), defined as the energy content of the fuel, was also measured. In the present study, the blends have LHV values similar to those of diesel fuel.

### 2.3. Experimental Engine Test

The tests were carried out on a LISTER-PETTER engine test bench at the IMT Atlantique laboratory. It is single cylinder with an output power of 4.5 kW at 1500 rpm. The engine is connected to an automatically controlled eddy current dynamometer. To analyze the combustion and the pollutant emissions, the engine test bench is equipped with several instruments, such as an exhaust gas analyzer, flow meters, thermocouples, pressure sensors, etc. Figure 2 illustrates the experimental setup. More details about instrumentation and data acquisition system were reported in our previous works [34,35]. Measurements of in-cylinder pressure from 100 consecutive cycles were recorded at a sampling interval of 0.2 crank angle (CA). The injection timing is fixed at 13 °CA before top dead center (TDC), as mentioned in the specifications of the manufacturer. The engine was calibrated before starting the test series. Experiments have been carried out at 25, 50, 75 and 100% full load, at a constant engine speed of 1500 rpm.



- |                          |                                  |
|--------------------------|----------------------------------|
| 1. Test engine           | 11. Fast data acquisition system |
| 2. Dynamometer           | 12. Slow data acquisition system |
| 3. Gaseous fuel supply   | 13. Cylinder pressure sensor     |
| 4. Gasoil tank           | 14. Injection pressure sensor    |
| 5. A/D card for pressure | 15. Liquid fuel filter           |
| 6. A/D card for Analyzer | 16. Gaseous fuel flow mete       |
| 7. Air tank              | 17. TDC encoder                  |
| 8. Air-gas Mixer         | 18. Speed sensor                 |
| 9. Diesel flow meter     | 19. Exhaust gas analyzer         |
| 10. Charge Amplifier     | 20. Smoke meter                  |

**Figure 2.** Experimental engine setup.

Two systems are used for engine control and signal acquisition. The first system controls the engine test rig and is used to record measurements at low frequency (125 Hz), such as pressure and temperature in the intake manifold, torque, engine speed, as well as exhaust emissions. The second data acquisition system measures high-frequency signals (90 kHz) such as cylinder pressure, injection pressure and crankshaft angular position. Cylinder pressure data was measured over 100 cycles at a sampling interval of 0.2 degrees crank angle (CA) using a water-cooled piezoelectric pressure sensor (AVL QH32D). A piezoelectric pressure transducer (AVL QH33D) is used to measure the injection pressure. It is located between the injection pump and the fuel injector. The crankshaft angular position is measured by an encoder (AVL 364C) placed on the flywheel. The air mass flow rate at the intake is measured by a differential pressure transmitter (LPX 5481), while the liquid fuel mass flow rate is measured using a Coriolis mass flowmeter (RHM015). Moreover, the test engine is equipped with a series of K-type thermocouples for temperature measurements. An exhaust gas analyser (crystal COSMA 500) placed on the exhaust manifold is used to measure the main pollutant gases ( $\text{NO}_x$ , CO, HC,  $\text{CO}_2$ ). Particulate emissions (PM) are measured using a particle sensor (type PPS-M). The particle sensor allows real-time, continuous and high-sensitivity measurements of raw exhausts PM emissions without diluting the exhaust gas. The engine specifications and the different types of sensors are shown in Tables 2 and 3 respectively. Uncertainty calculation is based on the method reported by Bora et al. [36].

**Table 2.** Specifications of Lister-Petter (TS1) engine.

Bore × stroke	95.3 mm × 88.9 mm
Cooling system	Air-cooled
Compression ratio	18:1
General details	4-Stroke, single cylinder, naturally aspirated,
Injection system	Direct injection
Orifices × diameter	4 × 0.25 mm
Connecting rod length	165.3 mm
Piston type	Cylindrical bowl (diameter: 45 mm and depth: 15 mm)
Displacement volume	630 cm <sup>3</sup>
injection timing	13° BTDC
injection pressure	240 bar
Rated power output	4.5 kW at 1500 rpm
EVO	76°CA BBDC
IVC	69°CA ABDC
IVO	36°CA BTDC
EVC	32°CA ATDC

**Table 3.** Accuracy and uncertainties of the measurements in the calculated results.

Measurements	Sensor Type	Accuracy
Torque	Effort sensor (FN 3148)	±0.1 N·m
Speed	AVL 365C	±3 rpm
Injection timing	AVL 365C	±0.05 °CA
Intake air flow rate	Differential pressure transmitter (LPX5841)	±1.0%
Temperature of exhaust gas	K type	±1.6 °C
Temperature of ambient air	HD 2012 TC/150	±0.2 °C
Temperature of injected fuel	K type	±1.6 °C
Cylinder pressure	Piezo-electric (AVL QH32D)	±2 bars
Injection pressure	Piezo-electric (AVL QH33D)	±2 bars
Fuel mass flow rate	Coriolis type (RHM015)(RHM015)	±0.5%

**Table 3.** *Cont.*

Measurements	Sensor Type	Accuracy
NO <sub>x</sub>	chemiluminescence (TOPAZE 32M)	±100 ppm
HC	FID (Graphite 52M)	±10 ppm
CO, CO <sub>2</sub> , O <sub>2</sub>	Infra-red detector (MIR 2M)	±50 ppm
Particulates	Electric (Pegasor Particle Sensor)	±1 µg/m <sup>3</sup>
Calculated results		Uncertainty range (%)
Air/Fuel equivalence ratio		1.1
BSFC		0.6–2.0
BTE		0.7–2.0
Brake power		0.4–1.9

#### 2.4. Model for Combustion Analysis

Before analyzing the combustion, it is important to process the pressure data. Indeed, the pressure data present a noisy tendency between successive values. In this study, smoothing was established using the smoothing equation for instantaneous pressure data used by several researchers reported in the literature [36].

Subsequently, the analysis of the combustion was performed by examining the heat release rate (HRR) which is determined by an analytical calculation model. The latter is based on the first law of thermodynamics and the ideal gas law. HRR depends on changes in cylinder pressure and combustion chamber volume [35,37]. It is calculated as follows in Equation (1):

$$dQ_{net}/d\theta = dQ_c/d\theta - dQ_w/d\theta = \gamma/(\gamma - 1) P [dV/d\theta] + \gamma/(\gamma - 1) V [dP/d\theta] \quad (1)$$

where  $dQ_{net}/d\theta$  is the net HRR,  $dQ_c/d\theta$  is the rate of heat released by the fuel combustion and  $dQ_w/d\theta$  is the heat transfer rate through the cylinder wall obtained from the Woschni correlation [37]. The  $\gamma$  is the specific heat ratio. According to the literature,  $\gamma$  is fixed at 1.35 [34]. The  $P$  is the cylinder pressure and  $V$  is the volume of the combustion chamber, which depends on the crankshaft angle ( $\theta$ ) and the geometric parameters of the engine. It is obtained in Equation (2) as shown below:

$$V(\theta) = V_d [(Cr/C_r - 1) - ((1 - \cos\theta)/2) + 1/2 ((2L/C)^2 - \sin^2\theta)]^{1/2} \quad (2)$$

where  $V_d$ ,  $C_r$ ,  $L$  and  $C$  are displacement, compression ratio, rod length and stroke, respectively.

### 3. Results and Discussion

In this part, we present the results of the different blends tested in terms of in-cylinder pressure, ignition delay (ID), HRR, polluting emissions and brake thermal efficiency compared with those of conventional diesel fuel at different loads. The engine speed and the injection timing are kept constant throughout the test's series at 1500 rpm and 13 °CA respectively.

#### 3.1. Combustion Characteristics

##### 3.1.1. Cylinder Pressure

The variation of the cylinder pressure during the engine cycle, as a function of crank angle, is illustrated in Figure 3. At medium load, it was noted that the curves coincide perfectly and tend to detach in the expansion phase. This could be explained by the difference in the combustion process during the diffusion phase and the thermal losses. At the same load, the peak cylinder pressure of the blends varies between 75 bars and 78 bars.

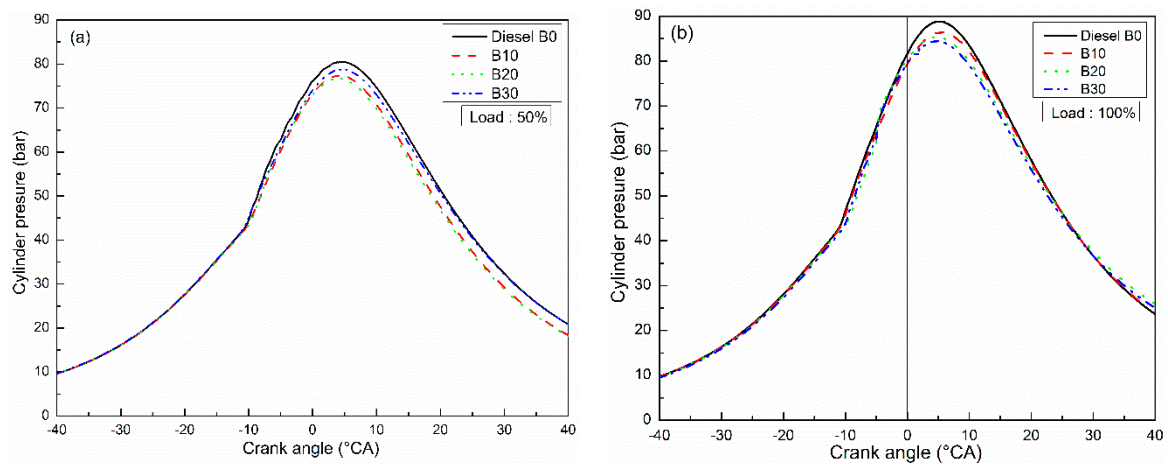


**Figure 3.** Cylinder pressure curves versus crank angle for diesel fuel and biofuel-diesel blends under medium (a) and full loads (b).

At full load, the B10 had a greater maximum cylinder pressure than that of B20 and B30 with a value of about 85 bars. Moreover, the cylinder pressure curve of the B10 was the closest to that of the diesel with a value of about 87 bars. The curves were similar during the three phases namely: the intake, the expansion and the exhaust phases.

This behavior could be explained by several parameters, such as viscosity, cetane number, the latent heat of vaporization and fuel oxygen content [38]. A combination of these factors can explain the behavior of in-cylinder pressure. In fact, it has been reported in the literature that the heat release rate depends on viscosity (affecting fuel atomization and vaporization) and latent heat of vaporization (directly affecting ignition delay and combustion cooling [39]). It is also important to note that there is no significant change in the position of the cylinder pressure peak. This information is essential to ensure the proper functioning of the engine. Indeed, for a maximum pressure in the immediate vicinity of TDC, the risk of degradation of engine performance is probable. Moreover, as reported by Nour et al. [40], the high cetane number and the low flash point lead to the reduction of the ignition delay, which consequently gives a lower cylinder pressure.

Moreover, the combustion efficiency was affected by the higher viscosity of biofuel, compared to that of diesel fuel, due to the bad fuel atomization, which leads to insufficient fuel-air blending. Therefore, since a lower proportion of fuel is burned in the premixing stage, more fuel is burned in the diffusion stage. This results in incomplete oxidation of unburned hydrocarbons before the exhaust valve opens [40].

### 3.1.2. Heat Release Rate (HRR)

As reported by Heywood [41], the combustion process in compression ignition engines is divided into three stages. It starts with ignition delay, followed by premixed combustion and finally diffusion combustion. Figure 4 depicts the evolution of the HRR versus the crank angle for the studied blends (B10, B20 and B30). Comparing the results with those for diesel fuel, it can be noted that higher HRR peaks are observed in the premixed phase of B20 at medium and high loads. This can be explained by the accumulation of fuel burned at a higher rate during the premixing phase of combustion, resulting in higher peak HRR values [41].

At full loads, the B30 exhibited the lowest HRR in the diffusion combustion phase among the tested blends. This is due to the worsening atomization of the tested fuel, which leads to inadequate fuel-air blending and therefore affects the combustion efficiency. Thus, more fuel is burnt in the diffusion combustion phase resulting in incomplete oxidation, of the unburned hydrocarbons before the exhaust valve opens, as reported by Nour et al. [40]. Moreover, at medium loads, the biofuels tested showed a similar HRR variation in the diffusion phase. On the other hand, the HRR curves are mostly similar during the first stage

of the combustion process, where a sharp increase in the rate of combustion is observed. Figure 5 presents the cumulative heat release (Figure 5a) and the combustion duration (Figure 5b) under different loads for all the tested fuels. It can be observed that B20 presents a higher cumulative heat release rate, while B10 showed a similar trend as diesel fuel (Figure 5a). The combustion duration is by definition, the period between the moment where the HRR takes a positive value and the moment at which 90% of the net heat is released, as reported in the literature [41]. It can be seen that the combustion duration of B30 is longer than that of the other fuels tested, at low and medium loads. However, at full loads, B20 showed a longer burn time than the other cases tested. Moreover, as observed in Figure 5a, the B20 has the highest cumulative heat release rate. In addition, the cumulative heat release rate of the B10 is similar to that of the B0.

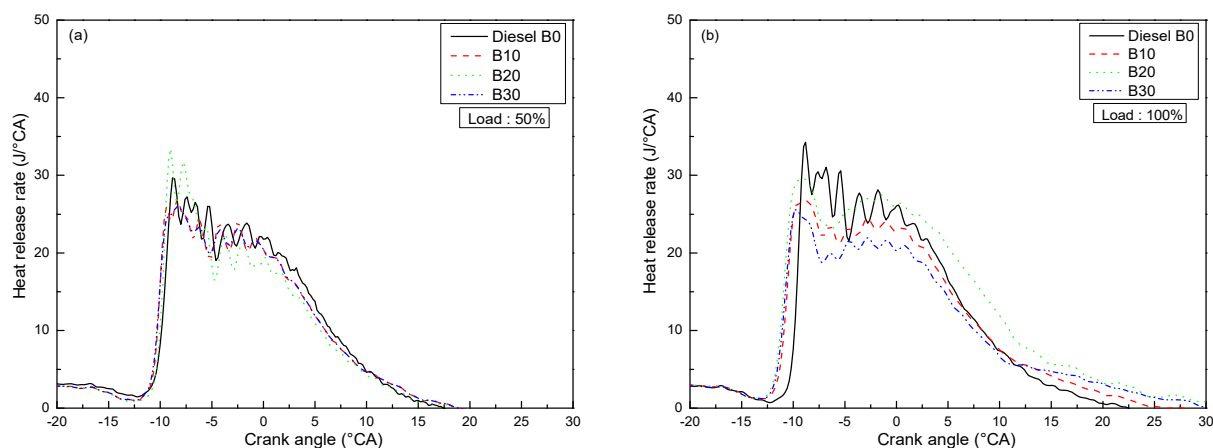


**Figure 4.** The heat release rate for diesel fuel and biofuel-diesel blends, (a) load 50%; (b) load 100%.

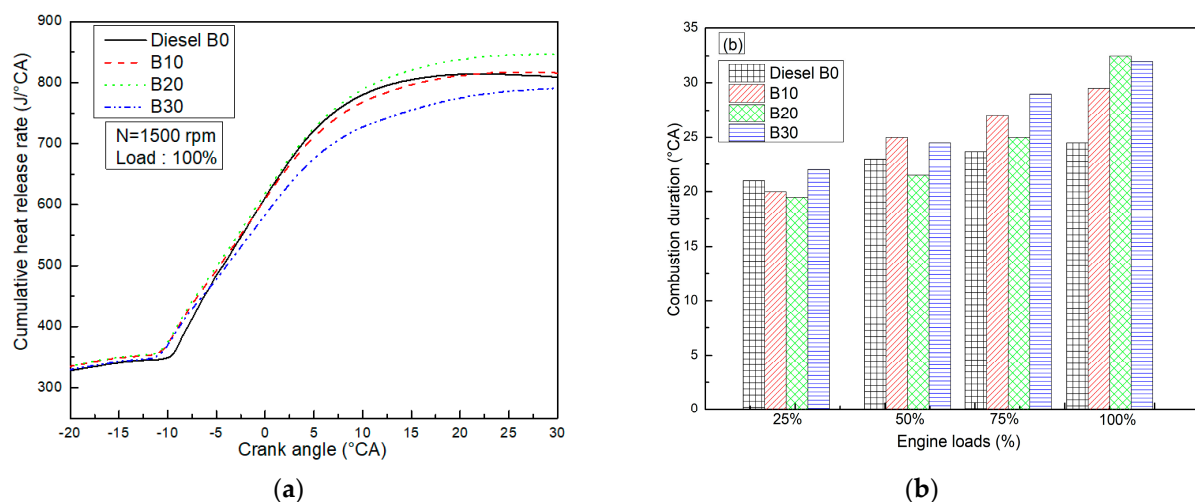


**Figure 5.** Cumulative heat release rate (a) and combustion duration (b) for diesel fuel and biofuel-diesel blends.

### 3.1.3. Ignition Delay

Figure 6 shows the change in ID as a function of the power output of the test fuel. From the literature, this parameter is the time interval from the start of fuel injection to the start of combustion. It participates in the analysis of combustion and explains the HHR behavior and of the cylinder pressure curves. It is composed of two periods: the physical delay period, where the air is blended with the fuel, during which air mixes with the fuel during atomization, vaporization, and the chemical lag time, which is the time it takes for the reactive combustion to start [37].

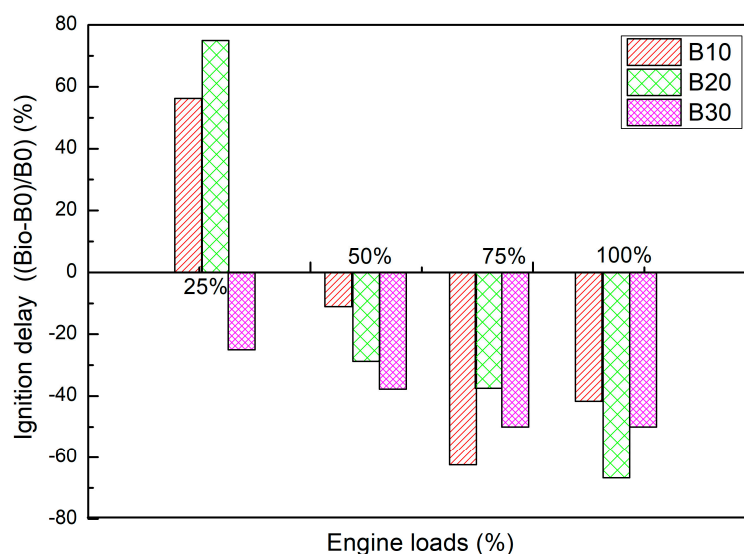


**Figure 6.** Ignition delay relative variation versus power output.

At medium and high loads, it was noticed that diesel fuel had a longer ID in comparison with that of the blends tested. It could be explained by the low flash point of diesel fuel (67 °C), compared to that of the biofuels blended tested, which is between 71 °C and 74 °C (as mentioned previously in Figure 1). Indeed, as reported by Rodica Niculescu et al. [39], the components in biodiesel blends boil at higher temperatures than conventional diesel fuel. Moreover, the conditions prevailing in the combustion chamber (pressure, temperature, equivalence ratio, etc.) could be responsible for the lower ID of blends. The same observation was observed by Piotr Łagowski et al. [42]. It appears that, when burning biodiesel blends, the heat release rate and cylinder pressure values are lower than diesel fuel alone. It can be explained by the shorter ID and lower fuel consumption.

Indeed, due to the increase in cylinder temperature and pressure and the equivalence ratio of the mixture, the ID decreased with increasing load. B30 presented a lower ID at all loads in comparison to diesel fuel.

Increasing the concentration of the biofuel in the blend accelerates and improves the vaporization of the fuel studied and enhances the fuel-air blend. However, a longer ID leads to an improvement in the second stage of HHR and higher cylinder temperature and pressure [40], as presented in Figures 3 and 4.

### 3.2. Engine Performance

BTE can be calculated by the following Equation (3):

$$\text{BTE} = P_{\text{out}} / (m_f \text{ LHV}_f) \quad (3)$$

where  $P_{\text{out}}$  is the brake power output.  $m_f$  and  $\text{LHV}_f$  are the mass flow rate and the lower heating value of the fuel respectively.

Figure 7 depicts the variation of BTE of biodiesel, with engine load at speed of 1500 rpm, in comparison to that of diesel fuel. It can be observed that blending biofuel with diesel leads to a decrease in BTE. B30 resulted in the highest decrease of approximately 10% followed by B20 with 7%. EL Kassaby et al. [43], reported the same observation. It turned out that the BTE of all biofuel blends was lower than that of pure diesel. Their study was based on the operation of the engine running with cooking oil, for different mixtures (B10, B20, B30 and B50). Also, it can be noticed from Figure 7 that B10 has a better efficiency compared to that of B20 and B30, for all the loads studied. Effectively, the BTE of B10 is close to that of diesel, with a maximum deviation of approximately 2.5%. This can be explained by a better combustion efficiency for B10 as it is shown by the pollutant emissions, especially CO and particulate matter, presented in the next section. On the other

hand, Panwar et al. [44], have carried out a performance test on different biofuel blends at a constant speed of 1500 rpm at various loads. It was concluded that the blends containing lower fractions of biodiesel reduced fuel consumption and improved BTE, which is observed in the present study. Moreover, the effects of injection time and injection pressure on the performance and emission characteristics, of DI diesel engines using methanol (5%, 10%, and 15%) as blended diesel fuel, were studied by Tanwar et al. [45]. The results showed that the proportion of methanol in the fuel mixture increased, as BTE decreases.

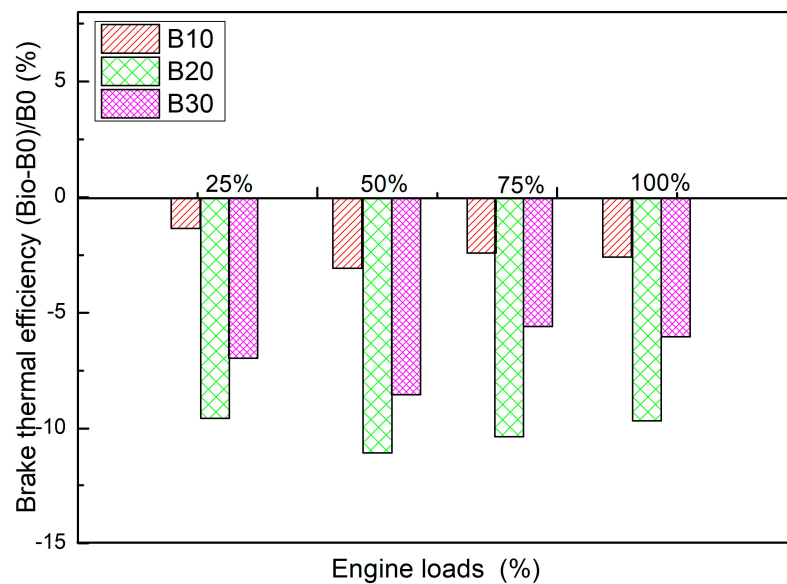


**Figure 7.** Evolution of the relative BTE versus power output.

### 3.3. Exhaust Emissions

#### 3.3.1. HC and CO Emissions

Figure 8 shows the relative variations of the concentration of HC and CO in the exhaust gas, as a function of the engine load, compared to diesel fuel. According to the literature [37], the emissions of HC and CO occur as a result of incomplete fuel combustion. It can be noticed from Figure 8a, that the blends emit lower concentrations of HC in comparison to diesel fuel. Moreover, at low loads, it was observed that HC emissions were almost the same for the different cases studied.

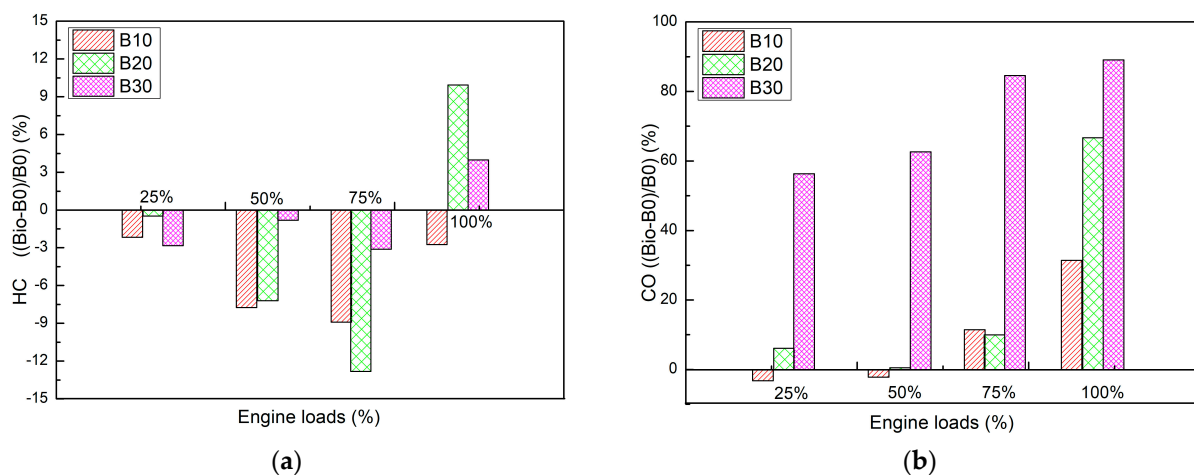


**Figure 8.** Variation of HC emissions (a) and CO emissions (b) versus loads.

At 50% of full load, B10 and B20 exhibited the minimum HC emissions, unlike B30. The opposite case was observed at full load, where B20 was the most polluting with a

percentage of 10% compared to that of diesel, while B10 was the least polluting blend. Di Y et al. [46], have observed the same behavior. Indeed, their study showed that by using 3% to 5% of their biodiesel, a slight decrease in HC emissions, compared to diesel fuel, was noted, while a blend of 15% to 25% of biodiesel exhibited a contradictory behavior. This difference can be attributed to a lower volatility of biodiesel than that of diesel fuel. In addition, Cheung CS et al. [47], reported that the reduction in HC emissions from biofuel, compared to diesel is due to the presence of an oxygen concentration in alcohol-biofuel-diesel blends, which induces a more complete combustion. At full load, HC emissions increase for B20 and B30 due to late combustion, as discussed previously for heat release analysis, which is in agreement with results found in the literature [48,49].

Figure 8b shows that in the case of low and medium loads, the CO emissions have almost the same concentration in the exhaust gases, as those of pure diesel, except B30. Indeed, a strong increase in CO emissions was recorded for B30, under all load conditions compared to the other cases studied. This incomplete combustion is due to a poor air-fuel mixture and lower reactivity [50]. Also, as reported by Çakmak A et al. [51], the increase in the concentration of CO emissions can be explained by the poor volatility and higher viscosity. This reasoning is reinforced by the increase in particulate emissions, as shown in the next section. In addition, this figure shows that the concentration of CO emissions of B10 was the lowest of those recorded for the other biofuels tested (B20 and B30), at high loads. This partly explains the good performance in terms of BTE of B10. Panua et al. [52], have obtained the same results, as the present study by concluding that the CO emissions were very close to those of diesel for low biodiesel blends.

### 3.3.2. NO<sub>x</sub> and Particulates Emissions

Figure 9 illustrates that the concentration of NO<sub>x</sub> emissions, from B20 and B10, is close to that of diesel for all the loads studied, except for the B30 fuel, which is considered the least polluting fuel in terms of NO<sub>x</sub>. A reduction of about 15–20% was noticed in comparison with that of diesel fuel. This can be explained by the reduction of combustion temperature and free radical formation [53]. These results are in accordance with those of CO emissions as shown in Figure 8b. Indeed, Heywood et al. [41] have reported that NO<sub>x</sub> emissions and CO are inversely proportional. Also, Panua et al. [52], reported in their study that, at higher blend concentrations, NO<sub>x</sub> emissions and performance were lower than conventional diesel which is in good agreement with the present study.

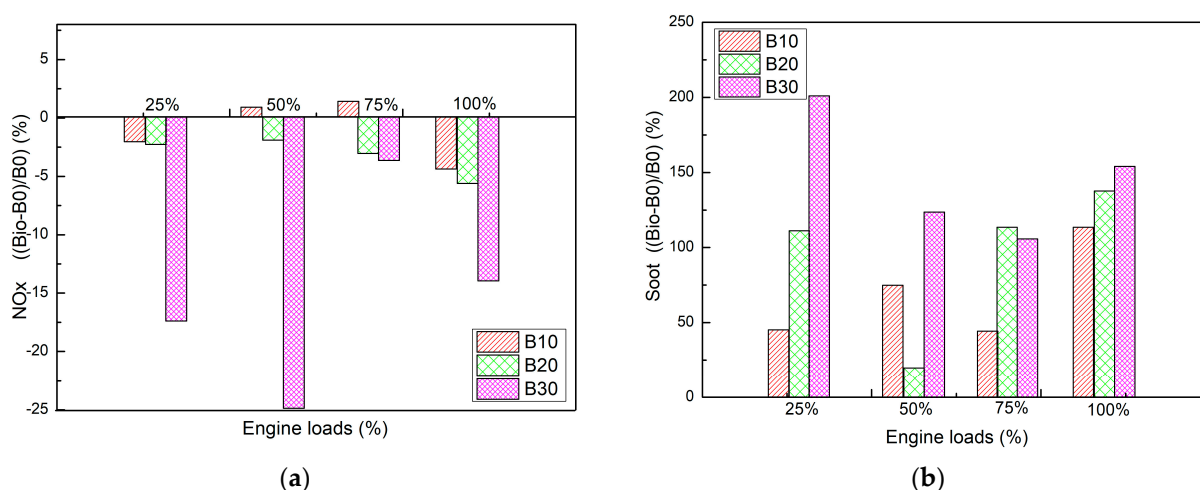


**Figure 9.** Variation of NO<sub>x</sub> emissions (a) and particulates emissions (b) versus loads.

Figure 9b presents the variation of particulate emissions. The results show an increase in these emissions for all the blends in comparison to diesel fuel. It can be clearly seen that B10 emits fewer particles than B20 and B30. As a reminder, one of the main factors of PM formation is the composition of the fuel used. In fact, the C–C bond strongly favors

the production of this kind of emissions [41]. It can be noticed that PM emissions are similar at high loads while B30 results in higher emissions at low and medium loads. This is due to the increase in fuel viscosity for the higher blend ratio and hence resulted in the poor formation of air–fuel blends [53,54]. Indeed, Alagu et al. [54] found that at full load, biodiesel (B10 blend) had higher concentrations of soot emissions (52.8%) than when operating with fossil diesel. This is due to the highest viscosity of fuel leading to worsening fuel atomization resulting in the formation of large droplet size.

#### 4. Conclusions

The focus of this study is the utilization of biofuel derived from wastewater generated by oil mills, specifically in diesel engines. Three proportions of biofuel (B10, B20 and B30) were tested in a single-cylinder diesel engine. A series of experimental engine tests were performed for different loads to thoroughly study the performance, combustion and pollutant emission characteristics of OMWW biofuel blends. From the engine tests, the following conclusions were drawn:

- Under full load conditions, the cylinder pressure curve of B10 closely resembled that of diesel, with a maximum value of 87 bars.
- The results showed that B10 leads to better performance compared to the other blends. This is due to several parameters such as better fuel atomization and low viscosity.
- At high loads, a reduction of 26% of CO emissions, and 11% of HC as well as PM emissions, were observed by using B10 blend in comparison with the B20 blend. In addition, a 10% improvement in brake thermal efficiency was noted.
- At high loads, B10 exhibits lower polluting effects than B30, with reductions of 43% in CO emissions, 10% in HC emissions, and 20% in particulate matter emissions.

Furthermore, even if the use of the other two biofuels, namely B20 and B30, is not efficient and less clean compared to B10, they remain very interesting because they are produced from waste.

**Author Contributions:** Conceptualization, F.Z.A., L.H. and K.L.; methodology, F.Z.A., L.H. and K.L.; validation, M.T. and K.L.; formal analysis, F.Z.A. and L.H.; investigation, F.Z.A. and L.H.; data curation, F.Z.A. and L.H.; writing—original draft preparation, F.Z.A. and L.H.; writing—review and editing M.T. and K.L.; supervision, M.T. and K.L. All authors have read and agreed to the published version of the manuscript.

**Funding:** This research received no external funding.

**Data Availability Statement:** Not applicable.

**Conflicts of Interest:** The authors declare no competing interests.

#### Nomenclature

P	Cylinder pressure, [bar]
V	Cylinder volume, [m <sup>3</sup> ]
$\gamma$	The ratio of specific heats, [-]
OMWW	Olive mill wastewater
Q	Heat, [J]
BTE	Brake thermal efficiency, [%]
HTL	Hydrothermal liquefaction
LHV	Lower heating value, [MJ]/kg]
$\dot{m}$	Mass flow rate, [kg/s]
HHV	Higher heating value, [MJ]/kg]
ID	Ignition delay, [deg CA]
P <sub>b</sub>	Brake power, [kW]

L	Connecting rod length, [m]
TDC	Top dead center
BDC	Bottom dead center
$V_d$	Displacement volume, [m]
$\theta$	Crank angle, [deg CA]
B0	100% diesel
CA	Crank angle
CI	Compression ignition
CO <sub>2</sub>	Carbon dioxide
C	Stroke, [m]
PM	Particulate matter
HC	Hydrocarbon
B10	Biofuel blends of 10% by volume of biofuel
B20	Biofuel blends of 20% by volume of biofuel
B30	Biofuel blends of 30% by volume of biofuel
CR	Compression ratio
NO <sub>x</sub>	Nitrogen oxides
CO	Carbon monoxide
Subscripts	
$w$	Wall of cylinder
$c$	Combustion
$b$	Brake

## References

- Hossain, F.M.; Kosinkova, J.; Brown, R.J.; Ristovski, Z.; Hankamer, B.; Stephens, E.; Rainey, T.J. Experimental Investigations of Physical and Chemical Large Batch Reactor. *Energies* **2017**, *10*, 467. [\[CrossRef\]](#)
- Hossain, F.M.; Nabi, N.; Rahman, M.; Bari, S.; Suara, K.; Ristovski, Z.; Brown, R.J. Experimental Investigation of Diesel Engine Performance, Combustion and Emissions Using a Novel Series of Dioctyl Phthalate (DOP) Biofuels Derived from Microalgae. *Energies* **2019**, *12*, 1964. [\[CrossRef\]](#)
- Kaur, R.; Gera, P.; Jha, M.K.; Bhaskar, T. Reaction Parameters Effect on Hydrothermal Liquefaction of Castor (*Ricinus Communis*) Residue for Energy and Valuable Hydrocarbons Recovery. *Renew. Energy* **2019**, *141*, 1026–1041. [\[CrossRef\]](#)
- Coyle, W.T. The future of biofuels: A global perspective. *J. Rural. Ment. Health* **2007**, *5*, 24–29. [\[CrossRef\]](#)
- Matayeva, A.; Bianchi, D.; Chiaberge, S.; Cavani, F.; Basile, F. Elucidation of reaction pathways of nitrogenous species by hydrothermal liquefaction process of model compounds. *Fuel* **2019**, *240*, 169–178. [\[CrossRef\]](#)
- Espadas-Aldana, G.; Vialle, C.; Belaud, J.P.; Vaca-Garcia, C.; Sablayrolles, C. Analysis and trends for Life Cycle Assessment of olive oil production. *Sustain. Prod. Consum.* **2019**, *19*, 216–230. [\[CrossRef\]](#)
- El Hassani, F.Z.; Fadile, A.; Faouzi, M.; Zinedine, A.; Merzouki, M.; Benlemlih, M. The long term effect of Olive Mill Wastewater (OMW) on organic matter humification in a semi-arid soil. *Heliyon* **2020**, *6*, e03181. [\[CrossRef\]](#)
- Romeo, R.; De Bruno, A.; Imeneo, V.; Piscopo, A.; Poiana, M. Impact of Stability of Enriched Oil with Phenolic Extract from Olive Mill Wastewaters. *Foods* **2020**, *9*, 856. [\[CrossRef\]](#)
- Hadhoum, L.; Burnens, G.; Loubar, K.; Balistrou, M.; Tazerout, M. Bio-oil recovery from olive mill wastewater in sub-/supercritical alcohol- water system. *Fuel* **2019**, *252*, 360–370. [\[CrossRef\]](#)
- Kipçak, E.; Söğüt, O.Ö.; Akgün, M. Hydrothermal gasification of olive mill wastewater as a biomass source in supercritical water. *J. Supercrit. Fluids* **2011**, *57*, 50–57. [\[CrossRef\]](#)
- Vitolo, S.; Petarca, L.; Bresci, B. Treatment of olive oil industry wastes. *Bioresour. Technol.* **1999**, *67*, 129–137. [\[CrossRef\]](#)
- Miranda, T.; Esteban, A.; Rojas, S.; Montero, I.; Ruiz, A. Combustion analysis of different olive residues. *Int. J. Mol. Sci.* **2008**, *9*, 512–525. [\[CrossRef\]](#) [\[PubMed\]](#)
- Poerschmann, J.; Baskyr, I.; Weiner, B.; Koehler, R.; Wedwitschka, H.; Kopinke, F.D. Hydrothermal carbonization of olive mill wastewater. *Bioresour. Technol.* **2013**, *133*, 581–588. [\[CrossRef\]](#)
- Peterson, A.A.; Vogel, F.; Lachance, R.P.; Fröling, M.; Antal, M.J.; Tester, J.W. Thermochemical biofuel production in hydrothermal media: A review of sub- and supercritical water technologies. *Energy Environ. Sci.* **2008**, *1*, 32–65. [\[CrossRef\]](#)
- Hadhoum, L.; Loubar, K.; Paraschiv, M.; Burnens, G.; Awad, S.; Tazerout, M. Optimization of oleaginous seeds liquefaction using response surface methodology. *Biomass Convers. Biorefinery* **2020**, *11*, 2655–2667. [\[CrossRef\]](#)
- Hadhoum, L.; Balistrou, M.; Burnens, G.; Loubar, K.; Tazerout, M. Hydrothermal liquefaction of oil mill wastewater for bio-oil production in subcritical conditions. *Bioresour. Technol.* **2016**, *218*, 9–17. [\[CrossRef\]](#)
- Haddad, K.; Jeguirim, M.; Jerbi, B.; Chouchene, A.; Dutournié, P.; Thevenin, N.; Ruidavets, L.; Jellali, S.; Limousy, L. Olive Mill Wastewater: From a Pollutant to Green Fuels, Agricultural Water Source and Biofertilizer. *ACS Sustain. Chem. Eng.* **2017**, *5*, 8988–8996. [\[CrossRef\]](#)

18. Elleuch, A.; Halouani, K.; Li, Y. Investigation of direct-fed Solid Oxide Fuel Cell fueled by upgraded bio-oil extracted from olive waste pyrolysis: Part 1: Bio-oil characterization and preliminary cell testing. *Energy Technol.* **2018**, *300072*, 53–60. [[CrossRef](#)]
19. Wu, X.; Daniel, R.; Tian, G.; Xu, H.; Huang, Z.; Richardson, D. Dual-injection: The flexible, bi-fuel concept for spark-ignition engines fuelled with various gasoline and biofuel blends. *Appl. Energy* **2011**, *88*, 2305–2314. [[CrossRef](#)]
20. Giakoumis, E.G.; Rakopoulos, C.D.; Dimaratos, A.M.; Rakopoulos, D.C. Exhaust emissions of diesel engines operating under transient conditions with biodiesel fuel blends. *Prog. Energy Combust. Sci.* **2012**, *38*, 691–715. [[CrossRef](#)]
21. Giakoumis, E.G.; Rakopoulos, D.C.; Rakopoulos, C.D. Combustion noise radiation during dynamic diesel engine operation including effects of various biofuel blends: A review. *Renew. Sustain. Energy Rev.* **2016**, *54*, 1099–1113. [[CrossRef](#)]
22. Abed, K.A.; Gad, M.S.; El Morsi, A.K.; Sayed, M.M.; Elyazeed, S.A. Effect of biodiesel fuels on diesel engine emissions. *Egypt. J. Pet.* **2019**, *28*, 183–188. [[CrossRef](#)]
23. Komninos, N.P.; Rakopoulos, C.D. Modeling HCCI combustion of biofuels: A review. *Renew. Sustain. Energy Rev.* **2012**, *16*, 1588–1610. [[CrossRef](#)]
24. Giakoumis, E.G. A statistical investigation of biodiesel effects on regulated exhaust emissions during transient cycles. *Appl. Energy* **2012**, *98*, 273–291. [[CrossRef](#)]
25. Debnath, B.K.; Sahoo, N.; Saha, U.K. Adjusting the operating characteristics to improve the performance of an emulsified palm oil methyl ester run diesel engine. *Energy Convers. Manag.* **2013**, *69*, 191–198. [[CrossRef](#)]
26. Karthikeyan, S.; Periyasamy, M.; Prathima, A.; Sabariswaran, K. Performance analysis of diesel engine fueled with *S. marginatum* Macro algae biofuel—Diesel blends. *Mater. Today Proc.* **2020**, *33*, 3464–3469. [[CrossRef](#)]
27. Kumar, P.S.; Donga, R.K.; Sahoo, P.K. Experimental comparative study between performance and emissions of jatropha biodiesel and diesel under varying injection pressures. *Int. J. Eng. Sci. Emerg. Technol.* **2012**, *3*, 98–112.
28. Kuti, O.A.; Zhu, J.; Nishida, K.; Wang, X.; Huang, Z. Characterization of spray and combustion processes of biodiesel fuel injected by diesel engine common rail system. *Fuel* **2013**, *104*, 838–846. [[CrossRef](#)]
29. Nabi, M.N.; Rahman, M.M.; Islam, M.A.; Hossain, F.M.; Brooks, P.; Rowlands, W.N.; Tulloch, J.; Ristovski, Z.D.; Brown, R.J. Fuel characterisation, engine performance, combustion and exhaust emissions with a new renewable Licella biofuel. *Energy Convers. Manag.* **2015**, *96*, 588–598. [[CrossRef](#)]
30. Wong, P.K.; Ghadikolaie, M.A.; Chen, S.H.; Fadairo, A.A.; Ng, K.W.; Lee, S.M.Y.; Xu, J.C.; Lian, Z.D.; Li, S.; Wong, H.C.; et al. Physicochemical and cell toxicity properties of particulate matter (PM) from a diesel vehicle fueled with diesel, spent coffee ground biodiesel, and ethanol. *Sci. Total Environ.* **2022**, *824*, 153873. [[CrossRef](#)]
31. Altarazi, Y.S.M.; Abu Talib, A.R.; Yu, J.; Gires, E.; Abdul Ghafir, M.F.; Lucas, J.; Yusaf, T. Effects of biofuel on engines performance and emission characteristics: A review. *Energy* **2022**, *238*, 121910. [[CrossRef](#)]
32. Imdadul, H.K.; Masjuki, H.H.; Kalam, M.A.; Zulkifli, N.W.M.; Alabdulkarem, A.; Rashed, M.M.; Teoh, Y.H.; How, H.G. Higher alcohol-biodiesel-diesel blends: An approach for improving the performance, emission, and combustion of a light-duty diesel engine. *Energy Convers. Manag.* **2016**, *111*, 174–185. [[CrossRef](#)]
33. Imdadul, H.K.; Masjuki, H.H.; Kalam, M.A.; Zulkifli, N.W.M.; Alabdulkarem, A.; Rashed, M.M.; Ashraful, A.M. Influences of ignition improver additive on ternary (diesel-biodiesel-higher alcohol) blends thermal stability and diesel engine performance. *Energy Convers. Manag.* **2016**, *123*, 252–264. [[CrossRef](#)]
34. Aklouche, F.Z.; Loubar, K.; Bentebbiche, A.; Awad, S.; Tazerout, M. Experimental investigation of the equivalence ratio influence on combustion, performance and exhaust emissions of a dual fuel diesel engine operating on synthetic biogas fuel. *Energy Convers. Manag.* **2017**, *152*, 291–299. [[CrossRef](#)]
35. Aklouche, F.Z.; Loubar, K.; Bentebbiche, A.; Awad, S.; Tazerout, M. Predictive model of the diesel engine operating in dual-fuel mode fuelled with different gaseous fuels. *Fuel* **2018**, *220*, 599–606. [[CrossRef](#)]
36. Bora, B.J.; Saha, U.K.; Chatterjee, S.; Veer, V. Effect of compression ratio on performance, combustion and emission characteristics of a dual fuel diesel engine run on raw biogas. *Energy Convers. Manag.* **2014**, *87*, 1000–1009. [[CrossRef](#)]
37. Fayette Taylor, C. *Internal Combustion Engine in Theory and Practice: Combustion, Fuels, Materials, Design*; Revised; MIT Press: Cambridge, MA, USA, 1985; Volume 2. [[CrossRef](#)]
38. Gumus, M. A comprehensive experimental investigation of combustion and heat release characteristics of a biodiesel (hazelnut kernel oil methyl ester) fueled direct injection compression ignition engine. *Fuel* **2010**, *89*, 2802–2814. [[CrossRef](#)]
39. Niculescu, R.; Clenci, A.; Iorga-Siman, V. Review on the use of diesel-biodiesel-alcohol blends in compression ignition engines. *Energies* **2019**, *12*, 1194. [[CrossRef](#)]
40. Nour, M.; Attia, A.M.A.; Nada, S.A. Combustion, performance and emission analysis of diesel engine fuelled by higher alcohols (butanol, octanol and heptanol)/diesel blends. *Energy Convers. Manag.* **2019**, *185*, 313–329. [[CrossRef](#)]
41. Heywood, J.B. *Internal Combustion Engine Fundamentals*; Tata McGraw-Hill Education Private Limited: New Delhi, India, 2013.
42. Łagowski, P.; Wcisło, G.; Kurczyński, D. Comparison of the Combustion Process Parameters in a Diesel Engine Powered by Second-Generation Biodiesel Compared to the First-Generation Biodiesel. *Energies* **2022**, *15*, 6835. [[CrossRef](#)]
43. EL\_Kassaby, M.; Nemit\_allah, M.A. Studying the effect of compression ratio on an engine fueled with waste oil produced biodiesel/diesel fuel. *Alex. Eng. J.* **2013**, *52*, 1–11. [[CrossRef](#)]
44. Panwar, N.L.; Shrirame, H.Y.; Rathore, N.S.; Jindal, S.; Kurchania, A.K. Performance evaluation of a diesel engine fueled with methyl ester of castor seed oil. *Appl. Therm. Eng.* **2010**, *30*, 245–249. [[CrossRef](#)]

45. Tanwar, M.D.; Torres, F.A.; Alqahtani, A.M.; Tanwar, P.K.; Bhand, Y.; Doustdar, O. Promising Bioalcohols for Low-Emission Vehicles. *Energies* **2023**, *16*, 597. [[CrossRef](#)]
46. Di, Y.; Cheung, C.S.; Huang, Z. Experimental investigation on regulated and unregulated emissions of a diesel engine fueled with ultra-low sulfur diesel fuel blended with biodiesel from waste cooking oil. *Sci. Total Environ.* **2009**, *407*, 835–846. [[CrossRef](#)]
47. Cheung, C.S.; Zhu, L.; Huang, Z. Regulated and unregulated emissions from a diesel engine fueled with biodiesel and biodiesel blended with methanol. *Atmos. Environ.* **2009**, *43*, 4865–4872. [[CrossRef](#)]
48. Muralidharan, K.; Vasudevan, D. Performance, emission and combustion characteristics of a variable compression ratio engine using methyl esters of waste cooking oil and diesel blends. *Appl. Energy* **2011**, *88*, 3959–3968. [[CrossRef](#)]
49. Ashraful, A.M.; Masjuki, H.H.; Kalam, M.A.; Rizwanul Fattah, I.M.; Imtenan, S.; Shahir, S.A.; Mobarak, H.M. Production and comparison of fuel properties, engine performance, and emission characteristics of biodiesel from various non-edible vegetable oils: A review. *Energy Convers. Manag.* **2014**, *80*, 202–228. [[CrossRef](#)]
50. Emberson, D.R.; Wyndorps, J.; Ahmed, A.; Pires Bjørgen, K.O.; Løvås, T. Detailed examination of the combustion of diesel and glycerol emulsions in a compression ignition engine. *Fuel* **2021**, *291*, 120147. [[CrossRef](#)]
51. ÇAKMAK, A.; ÖZCAN, H. Evaluation of glycerol tert-butyl ethers as renewable fuel additive. *Int. J. Automot. Eng. Technol.* **2020**, *9*, 66–75. [[CrossRef](#)]
52. De, B.; Panua, R.S. An experimental study on performance and emission characteristics of vegetable oil blends with diesel in a direct injection variable compression ignition engine. *Procedia Eng.* **2014**, *90*, 431–438. [[CrossRef](#)]
53. Balaji, G.; Cheralathan, M. Experimental investigation of antioxidant effect on oxidation stability and emissions in a methyl ester of neem oil fueled DI diesel engine. *Renew. Energy* **2015**, *74*, 910–916. [[CrossRef](#)]
54. Alagu, R.M.; Sundaram, E.G. Preparation and characterization of pyrolytic oil through pyrolysis of neem seed and study of performance, combustion and emission characteristics in CI engine. *J. Energy Inst.* **2018**, *91*, 100–109. [[CrossRef](#)]

**Disclaimer/Publisher's Note:** The statements, opinions and data contained in all publications are solely those of the individual author(s) and contributor(s) and not of MDPI and/or the editor(s). MDPI and/or the editor(s) disclaim responsibility for any injury to people or property resulting from any ideas, methods, instructions or products referred to in the content.